MODELING A CLASS OF MULTI-PORT NONLINEARITIES IN WAVE DIGITAL STRUCTURES

A. Bernardini[§]*, K.J. Werner*[†]*, A. Sarti*[§]*, J.O. Smith*[†]

[§] Dipartimento di Elettronica,
Informazione e Bioingegneria (DEIB)
Politecnico di Milano
Piazza L. Da Vinci 32, 20133 Milano – Italy
alberto.bernardini@mail.polimi.it
augusto.sarti@polimi.it

[†] Center for Computer Research
in Music and Acoustics (CCRMA)
Stanford University
Stanford, California 94305-8180, USA
kwerner@ccrma.stanford.edu
jos@ccrma.stanford.edu

ABSTRACT

Wave Digital Structures (WDS) are particularly interesting for applications of interactive modeling of nonlinear (NL) elements in the context of Virtual Analog modeling. NL circuits, however, often include multiple nonlinearities or multi-port nonlinearities, which cannot readily be accommodated by traditional WDS. In this work we present a novel method for modeling in the WD domain a class of multi-port NL elements that are obtained as the interconnection of linear and NL resistive bipoles. Our technique is based on a Piece-Wise Linear approximation of the individual bipoles that constitute the multi-port element. The method generalizes the existing solutions that are available in the literature as it enables the modeling of arbitrary interconnections between outer ports of the nonlinearity and individual ports of the local NL bipoles.

Index Terms— Circuit simulation, physical modeling sound synthesis, non linear signal processing, wave digital filters

1. INTRODUCTION

Wave Digital Filters (WDFs) [1] were originally aimed at designing digital filters that closely match the behaviour of analog reference circuits. Their design is based on a port-wise consideration of the reference circuit (one-port elements and topological "adaptors"), a linear transformation of Kirchhoff (K) variables (voltage and current) to pairs of waves (incident and reflected), and discretization of reactive circuit elements via the bilinear transform [2]. WDFs originally focused only on linear circuits, but their use was later extended to nonlinear circuit modeling. NL WDFs are particularly interesting in the context of Sound Synthesis through physical modeling [3], and Virtual Analog processing [4]. Initial theoretical work focused on one-port nonlinearities with DC descriptions [5, 6]; this was later expanded to consider nonlinearities with memory [3, 7, 8]. For reasons of realizability, it is usually not possible to include more than a single NL Element (NLE) in a WDF. In some special cases, techniques exist for lumping multiple NLEs into a single one-port NLE [9]. In other cases, known properties of the NLE can be used to produce approximations to multi-port NLEs with a single port and cross-control [4, 10] or solution schemes that are customized to a particular NLE [11]. There are only a few general approaches to accommodate multi-port NLEs or multiple NLEs. Recent work by Schwertdfeger and Kummert leverages contractivity properties of WDFs to solve the realizability problem through iteration (framed as an extension of time to an extra dimension) [12]. Earlier work by Petrausch and Rabenstein focused on a vector treatment of multiple single-port NL bipoles using multi-port WDFs [13]. In this work we focus on a class of multi-port NLEs, which is defined as an arbitrary interconnection of NL resistive bipoles. The port variables of such multi-port elements, therefore, are functions of the port variables of the local NL bipoles. This class of multi-port elements, in fact, is more general than those implemented in the literature using Piece-Wise Linear (PWL) approaches [13], and it enables the emulation of a wider family of NL circuits in the WD domain. Section 2 describes the necessary properties a generic multi-port NLE should have in order to obtain explicit wave scattering relations for each of its ports. In Section 3 we present the new class of multi-port PWL models and two significant parameterization strategies, which can be applied to such models in order to fulfill the mentioned properties of "explicitability". Section 4 describes two applications of PWL models. Section 5 concludes this paper.

2. MULTI-PORT NL WDFS

The transformation that maps K port variables onto WD port variables for a generic N-port element can always be written in matrix form [14] as

$$\begin{bmatrix} \mathbf{a} \\ \mathbf{b} \end{bmatrix} = \begin{bmatrix} \mathbf{E} & \mathbf{R} \\ \mathbf{E} & -\mathbf{R} \end{bmatrix} \begin{bmatrix} \mathbf{V} \\ \mathbf{I} \end{bmatrix} \quad , \tag{1}$$

978-0-9928626-3-3/15/$31.00 ©2015 IEEE

where $\mathbf{V} = [V_1, V_2, ..., V_N]^T$ is the vector of *across* K port variables; $\mathbf{I} = [I_1, I_2, ..., I_N]^T$ is the vector of *through* K port variables; $\mathbf{a} = [a_1, a_2, ..., a_N]^T$ and $\mathbf{b} = [b_1, b_2, ..., b_N]^T$ are the vectors of incident and reflected waves, respectively; $\mathbf{R} = \mathrm{diag}\,[R_{01}, R_{01}, ...R_{0N}]$ is the diagonal port resistance matrix; and $\mathbf{E}$ is the $(N \times N)$ identity matrix.

An explicit description based on waves for an N-port NLE can be readily obtained if we can find an appropriate parametric representation of the NL wave mappings. This was already discussed for the case of one-port NL bipoles without memory [5] and with memory [7]. Petrausch and Rabenstein presented a vector generalization of this parameterization in [13], which can be used for accommodating multiple NL bipoles in a WDF structure. That formulation employs a parameter vector α whose dimension matches the number of ports N of the NLE. In this paper we adopt a similar parameterization, whose vector $\alpha = [\alpha_1, \alpha_2, ..., \alpha_G]$ is assumed to have G independent variables, where $1 \leq G \leq N$. This allows us to express $\mathbf{V}$ or $\mathbf{I}$ or both of them as functions of α, $\mathbf{V} = f_V(\alpha)$, $\mathbf{I} = f_I(\alpha)$, and then to express also $\mathbf{a}$ and $\mathbf{b}$ as functions of α, $\mathbf{a} = f_a(\alpha)$, $\mathbf{b} = f_b(\alpha)$. In order to obtain explicit scattering relations in the WD domain, f_a must be invertible, which allows us to write

$$\mathbf{b} = \mathbf{b}\,(\mathbf{a}) = f_b\left(f_a^{-1}\,(\mathbf{a})\right) \quad . \tag{2}$$

In [13] the NL characteristics of the bipoles are sampled and turned into monotonic and continuous PWL characteristics. The coordinates of the sampled points, however, are exactly the variables $\mathbf{V}$ and $\mathbf{I}$, needed to determine $\mathbf{a}$ and $\mathbf{b}$ through (1). In the following section we will show how to generalize that approach, addressing NLEs where port variables may be functions of the other port variables and they are not necessarily the coordinates of the characteristics of the interconnected NL bipoles.

3. PWL MODELS

In this paper we consider PWL functions relating *across* and *through* variables (voltage v and current i) in NL bipoles. Such functions—which are assumed as being monotonic, continuous, and passing through the origin—are called *PWL resistances* as they consist of adjacent line segments sharing end-points. Fig.1, for example, shows the characteristic of a PWL resistance approximating a diode. We express a generic PWL resistance in the form

$$v = \lambda\,(i)\,i + q\,(i) \quad , \tag{3}$$

where $\lambda(i)$ and $q(i)$ are the current-controlled slope and v-intercept of the corresponding line segment. Because of the PWL nature of the characteristics, we can write $\lambda(i) = \lambda_k$ if $i_k \leq i < i_{k+1}$, k being an index ranging between the integers K^- and K^+ ($-K^- \leq k < K^+$). We assume that λ_k is the slope of the k-th segment joining $P_k = [i_k, v_k]$ and $P_{k+1} = [i_{k+1}, v_{k+1}]$. The end point $P_0 = [i_0, v_0]$ is conventionally picked as the origin of the axes. The total number of line segments is therefore $K = K^- + K^+$.

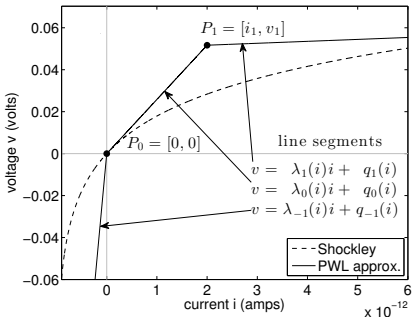

Fig. 1. A PWL resistance approximating a Shockley diode model

We have defined a current-controlled PWL resistance, but as we are dealing with monotonic characteristics, we could have just as easily expressed i as a PWL function of v.

There is a wide range of N-port NLEs that are made of $M \geq 1$ NL bipoles (e.g. diodes) interconnected with each other and with other linear components. In this work we focus on instantaneous (resistive) NLEs of the sort. We present models of such multi-port NLEs, which approximate the M NL characteristics of the NL bipoles with PWL resistances. We call such models *PWL models*. A PWL model permits instantaneous description of the N-port NLE using a linear system of equations. The total number of such linear systems is equal to the number of possible combinations of line segments (*CMBs*), considering all the PWL resistances of the NLE. Letting K_m be the number of line segments of the m-th PWL resistance, with $1 \leq m \leq M$, we can compute the total number of CMBs as $\prod_{m=1}^{M} K_m$.

A combination of points P_m (one per PWL resistance), represented by the vector $\mathbf{i} = [i_1, i_2, ..., i_M]^T$ or $\mathbf{v} = [v_1, v_2, ..., v_M]^T$, can be projected to a point $\mathbf{I}$ of the vector space of port currents, or in a point $\mathbf{V}$ of the vector space of port voltages. The projection can be performed using the most convenient (least complex) of the following four geometric transformations

$$\begin{array}{ll} \mathbf{I} = \mathbf{H_1 i} + \mathbf{H_{01}} & \mathbf{I} = \mathbf{H_2 v} + \mathbf{H_{02}} \\ \mathbf{V} = \mathbf{H_3 v} + \mathbf{H_{03}} & \mathbf{V} = \mathbf{H_4 i} + \mathbf{H_{04}} \end{array} \tag{4}$$

where the entries of the $(N \times M)$ matrices $\mathbf{H_1}$, $\mathbf{H_2}$, $\mathbf{H_3}$, $\mathbf{H_4}$ are scalar functions of the M slopes $\lambda_m\,(i_m)$, with $1 \leq m \leq M$, while $\mathbf{H_{01}}$, $\mathbf{H_{02}}$, $\mathbf{H_{03}}$, $\mathbf{H_{04}}$ are scalar vector functions of the slopes and the intercepts $q_m\,(i_m)$. When applying the transformation (4), we should remember that slopes and intercepts have piece-wise fixed values. In particular, they are the parameters of the segments of the PWL resistances.

Through linear systems of equations we can derive explicit vector expressions relating the vector variables $\mathbf{a}$ and

$\mathbf{b}$. As mentioned in section II explicit one-to-one wave mappings are granted only if a proper α-parameterization is performed and (2) holds. The choice of the most suitable parameterization is done according to which of the four (4) transformations had been applied and checking the K port variables dependences. Hereafter we propose two possible parameterizations, which can be generally applied. The two parameterizations are performed using two different, though analogous, procedures.

The first procedure consists in considering the system of equations in the K domain describing the NLE of interest and substituting each port current I_n $(1 \leq n \leq N)$ with the following expression derived from (1)

$$I_n = \frac{a_n - V_n}{R_{0n}} \ . \tag{5}$$

Solved the new resulting system of linear equations having port voltages as unknowns, we can write the following affine transformation in matrix form

$$\mathbf{V} = \mathbf{F_V a} + \mathbf{F_{0V}} \ , \tag{6}$$

where the entries of the square matrix $\mathbf{F_V}$, f_{jn}, with $j, n \in [1, N] \subseteq \mathbb{N}$, are scalar functions of the M slopes $\lambda_m\,(i_m)$, while the elements of the vector $\mathbf{F_{0V}}$, f_{0n}, are scalar functions of the slopes and the M intercepts functions $q_m\,(i_m)$. Obviously each f_{jn} depends also on the port reference resistances R_{0n}. The maximum number G of independent variables of $\mathbf{V}$ may be the proper size of the vector parameter α. Setting $\mathbf{V} = \alpha_\mathbf{V}$ with $\alpha_\mathbf{V} = [\alpha, V_{G+1}, V_{G+2}, ..., V_N]^T$, we can write

$$\alpha_\mathbf{V} = \mathbf{F_V a} + \mathbf{F_{0V}} \ . \tag{7}$$

Naming $f_a(\alpha)^{-1}$ the function (7), we can find an explicit inverse function $\mathbf{a} = f_a(\alpha)$, starting from the expression

$$\mathbf{F_V a} = \alpha_\mathbf{V} - \mathbf{F_{0V}} \ , \tag{8}$$

only if the matrix $\mathbf{F_V}$ is invertible (full rank); otherwise we have to search the set of incident wave vectors $\mathbf{a}$ satisfying (8). As the entries of $\mathbf{F_V}$ change at each time step, we have to check which relations exist among the entries of different rows and, if possible, we set the necessary algebraic constraints on the slopes in order to guarantee that the matrix will always be full rank. Then substituting $\mathbf{V} = \alpha_\mathbf{V}$ in the following matrix relation, derived from (1),

$$\mathbf{b} = 2\mathbf{V} - \mathbf{a} \ , \tag{9}$$

we obtain an explicit wave mapping in the form (2)

$$\mathbf{b} = (2\mathbf{F_V} - \mathbf{E})\,\mathbf{a} + 2\mathbf{F_{0V}} \ . \tag{10}$$

The second parameterization is performed similarly. Firstly, we substitute each port voltage V_n in the system of equations in the K domain with the expression

$$V_n = a_n - R_{0n} I_n \ . \tag{11}$$

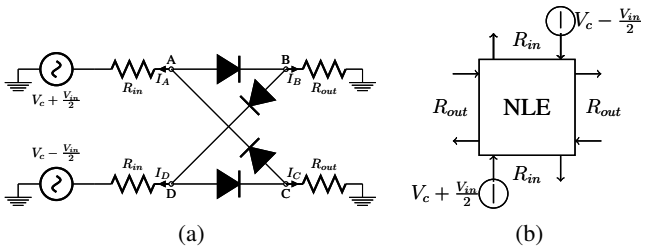

Fig. 2. Transformer-less ring modulator (a) and its WD implementation (b).

Solved the resulting system of linear equations having port currents as unknowns and set $\mathbf{I} = \alpha_\mathbf{I}$ with $\alpha_\mathbf{I} = [\alpha, I_{G+1}, I_{G+2}, ..., I_N]^T$, we can write

$$\alpha_\mathbf{I} = \mathbf{F_I a} + \mathbf{F_{0I}} \ , \tag{12}$$

where the entries of $\mathbf{F_I}$ are again functions of the slopes and the entries of the vector $\mathbf{F_{0I}}$ are functions of the slopes and the intercepts. Naming $f_a(\alpha)^{-1}$ the function (12), we can find an explicit inverse function $\mathbf{a} = f_a(\alpha)$, starting from the expression

$$\mathbf{F_I a} = \alpha_\mathbf{I} - \mathbf{F_{0I}} \ , \tag{13}$$

only if the matrix $\mathbf{F_I}$ is full rank. Substituting $\mathbf{I} = \alpha_\mathbf{I}$ in the following matrix relation, derived from (1),

$$\mathbf{b} = \mathbf{a} - 2\mathbf{RI} \ , \tag{14}$$

we obtain an explicit wave mapping in the form (2)

$$\mathbf{b} = (\mathbf{E} - 2\mathbf{RF_I})\,\mathbf{a} - 2\mathbf{RF_{0I}} \ . \tag{15}$$

Using one of the two parameterizations described so far, we are able to map the sampled points of the line segments proper of a specific CMB in points belonging to defined regions of the incident waves vector space. We can accurately perform this mapping for all the CMBs only once and save the results in an ordered data structure. So, during a real time simulation, at each time step, we only need to perform a search algorithm in order to find the CMB corresponding to the instantaneous vector of incident waves. Then, identified the right CMB, we set the correct values of the slope functions λ_m and the intercepts q_m. Finally we are able to compute the reflected waves using (10) or (15).

4. EXAMPLES OF APPLICATIONS

In this section we present two examples of applications of PWL models. The first example is an implementation of a transformer-less ring modulator, whose model in Fig.2a was already proposed by Parker in [15]. V_{in} and V_c are the modulator and the carrier signals, respectively. In his paper, Parker performs a further simplification involving the elimination

of non-conducting diodes at each time instant, while in our model the four diodes are always present. We implement the NLE using four ports, $N = 4$, as shown in Fig.2b. The port voltages are potentials at the four terminals, A, B, C and D. The port currents exit through the four terminals, directed towards ground. We name the four ports according to the corresponding terminals, so we write the port variables as $\mathbf{V} = [V_A, V_B, V_C, V_D]^T$ and $\mathbf{I} = [I_A, I_B, I_C, I_D]^T$. Our definition of ports, exploiting ground as external reference potential, is analogous to the one made in [11], where a WD implementation of a 3-port triode is presented. As pointed out in [11], when all the ports have a common external prong, e.g. ground, since the incoming waves seen by the NLE are the outgoing waves from the subcircuits connected to it and vice versa, we need to "exchange the roles" of $\mathbf{a}$ and $\mathbf{b}$ in (1). The four identical diodes are approximated with $M = 4$ identical PWL resistances as the one shown in Fig.1. The real diode reference characteristic is described by the known Shockley model with saturation current $I_s = 10^{-12}$ amps, thermal voltage $V_t = 25.85$ mV and ideality factor $\eta = 2.19$. We write the i–v characteristic of the diode among terminals A and B as $v_{AB} = \lambda_{AB}(i_{AB})i_{AB} + q_{AB}(i_{AB})$. The same holds for the other three diodes. The slopes and end point coordinates of the approximating PWL characteristic are: $\lambda_{-1} = 2.585 \times 10^{11}$, $P_0 = (0, 0)$, $\lambda_0 = 2.585 \times 10^{10}$, $P_1 = (2{\times}10^{-12}, 0.0517)$, $\lambda_1 = 9.232{\times}10^{-8}$. It follows that, since each PWL characteristic has $K_m = 3$ line segments, with $1 \leq m \leq M$, the total number of possible CMBs will be $\prod_{m=1}^{M} K_m = 81$. A generic vector of M current values, one for each PWL resistance, $\mathbf{i} = [i_{AB}, i_{BD}, i_{CA}, i_{DC}]^T$, can be projected into the port currents vector space using the simple transformation

$$\mathbf{I} = \begin{bmatrix} -1 & 0 & 1 & 0 \\ 1 & -1 & 0 & 0 \\ 0 & 0 & -1 & 1 \\ 0 & 1 & 0 & -1 \end{bmatrix} \mathbf{i} \ . \tag{16}$$

The relationship between $\mathbf{I}$ and $\mathbf{V}$ is described by the following system of equations where the arguments of the slope and intercept functions are omitted for the sake of readability

$$\begin{cases} I_A = V_A \left(\frac{-1}{\lambda_{CA}} - \frac{1}{\lambda_{AB}}\right) + \frac{V_B}{\lambda_{AB}} + \frac{V_C}{\lambda_{CA}} - \frac{q_{CA}}{\lambda_{CA}} + \frac{q_{AB}}{\lambda_{AB}} \\ I_B = \frac{V_A}{\lambda_{AB}} + V_B \left(\frac{-1}{\lambda_{AB}} - \frac{1}{\lambda_{BD}}\right) + \frac{V_D}{\lambda_{BD}} - \frac{q_{AB}}{\lambda_{AB}} + \frac{q_{BD}}{\lambda_{BD}} \\ I_C = \frac{V_A}{\lambda_{CA}} + V_C \left(\frac{-1}{\lambda_{BD}} - \frac{1}{\lambda_{DC}}\right) + \frac{V_D}{\lambda_{DC}} - \frac{q_{DC}}{\lambda_{DC}} + \frac{q_{CA}}{\lambda_{CA}} \\ I_A + I_B + I_C + I_D = 0 \ . \end{cases} \tag{17}$$

We apply the second parameterization procedure described in section 3 to the system of equation (17). Since the roles of $\mathbf{a}$ and $\mathbf{b}$ are exchanged, the substitution (11) becomes

$$V_n = a_n + R_{0n} I_n \ . \tag{18}$$

Then we obtain a vector parameter satisfying equation (12) and we derive the mapping between the possible CMBs and the corresponding regions of incident waves vector space, using expression (13). Finally we find an explicit scattering wave relation in the form (15) with two changes of sign due to the inversion of waves roles

$$\mathbf{b} = (\mathbf{E} + 2\mathbf{R}\mathbf{F}_{\mathbf{I}})\,\mathbf{a} + 2\mathbf{R}\mathbf{F}_{\mathbf{OI}} \ . \tag{19}$$

We perform a simulation to test our WD implementation, using sinusoidal input signals; $V_{in}(t) = g_{in}(\sin(2\,\pi\,\frac{f_{0in}}{F_s}\,t))$ and $V_c(t) = g_c(\sin(2\,\pi\,\frac{f_{0c}}{F_s}\,t))$, with $g_{in} = 1$ V, $f_{0in} = 500$ Hz and $F_s = 96$ kHz. The other circuit parameters are $R_{in} = 80\,\Omega$, $g_c = 1$ V, $f_{0c} = 1500$ Hz and $R_{out} = 10^4\,\Omega$.

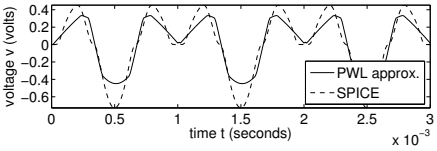

Fig. 3. Ring modulator: WD and SPICE simulations

The second proposed example of application is the implementation of a BJT amplifier in the simple common collector configuration represented in Fig.4, often also called "emitter follower". Setting $V_{bias} = 0$ V, only the positive part of the input signal V_{in} is "well-biased", while the negative part is flattened, hence the common collector amplifier can be used as an half wave rectifier. In this simulation we model the BJT using the classical Ebers Moll Model (EMM) introduced in [16]. The EMM characteristic equations are:

$$\begin{cases} I_E = i_{BE} - \alpha_r i_{BC} \\ I_C = i_{BC} - \alpha_f i_{BE} \\ I_E + I_B + I_C = 0 \ , \end{cases} \tag{20}$$

where I_E, I_C and I_B are the currents at the emitter, the collector and the base respectively, while i_{BE} and i_{BC} are the currents passing through the 2 diodes of the EMM, described using the Shockley model with $\eta = 1$, $I_s = 10^{-12}$ amps and $V_t = 25.85$ mV. We set the forward and reverse short circuit current gains to $\alpha_f = 0.89$ and $\alpha_r = 0.8$ respectively. We approximate the 2 diodes with $M = 2$ identical PWL resistances (e.g. $V_B - V_E = \lambda_{BE} i_{BE} + q_{BE}$), characterized by

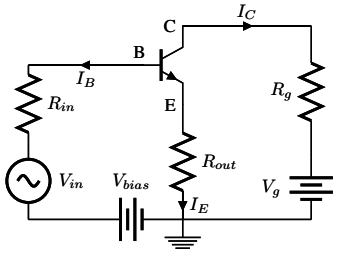

Fig. 4. Common collector BJT amplifier

$K_m = 2$ line segments each, having P_0 as common end point; the total number of possible CMBs will be $\prod_{m=1}^{M} K_m = 4$. The parameters of the PWL resistances are $\lambda_{-1} = 10^{-6}$ and $\lambda_0 = 5 \times 10^8$. We model the BJT as a 3-port NLE, $N = 3$; the corresponding port currents vector is $\mathbf{I} = [I_E, I_C, I_B]^T$ and the port voltage vector is $\mathbf{V} = [V_E, V_C, V_B]^T$. Also in this case the roles of $\mathbf{a}$ and $\mathbf{b}$ are exchanged, since the N ports have ground as common terminal. The matrix transformation between the vector of local currents, $\mathbf{i} = [i_{BE}, i_{BC}]^T$, and $\mathbf{I}$ is:

$$\mathbf{I} = \begin{bmatrix} 1 & -\alpha_r \\ -\alpha_f & 1 \\ (\alpha_f - 1) & (\alpha_r - 1) \end{bmatrix} \mathbf{i} \ . \tag{21}$$

In order to find an explicit wave mapping the second parameterization described in section 3 is applied. For the simulation we use a sinusoidal input signal $V_{in}(t) = g_{in}(\sin(2\,\pi\,\frac{f_{0in}}{F_s}\,t))$ with $g_{in} = 1.5$ V, $f_{0in} = 200$ Hz and $F_s = 44$ KHz. The other circuit parameters are: $R_{in} = 1\,\Omega$, $V_{bias} = 2$ V, $V_g = 15$ V, $R_g = 2\,\Omega$ and $R_{out} = 5000\,\Omega$. Fig.3 and Fig.5 show

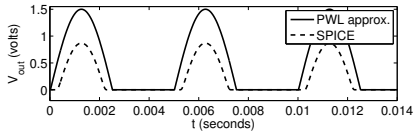

Fig. 5. BJT amplifier: WD and SPICE simulations

the comparisons between the output signals obtained using SPICE and the WD PWL models. The mismatches we notice are justified by the fact we are approximating each diode characteristic with only 3 line segments in the first case and 2 in the second case. However the PWL models grasp accurately the real circuits behavior.

5. CONCLUSIONS AND FUTURE RESEARCH

In this paper we have presented a new class of explicit PWL WD models of multi-port NLEs containing an arbitrary number of NL bipoles, forming any topological structure. The proposed models allow to accommodate multi-port NLEs, where each port variable is a NL function of all others ports' variables. In the future we aim to extend the presented approach to PWL resistances with more than two terminals and to NLEs with memory. Moreover we will search effective techniques to implement PWL resistances characterized by more line segments.

REFERENCES

[1] A. Fettweis, "Wave digital filters: Theory and practice," *Proc. IEEE*, vol. 74, no. 2, pp. 270–327, 1986.

[2] J.O. Smith, *Physical Audio Sig. Processing for Virtual Musical Instruments and Audio Effects*, 2010, online book.

[3] F. Pedersini, A. Sarti, and S. Tubaro, "Object-based sound synthesis for virtual environments-using musical acoustics," *IEEE Sig. Process. Magazine*, vol. 17, no. 6, pp. 37–51, Nov. 2000.

[4] G. De Sanctis and A. Sarti, "Virtual analog modeling in the wave-digital domain," *IEEE Trans. Audio, Speech, and Lang. Process.*, vol. 18, no. 4, pp. 715–727, May 2010.

[5] K. Meerkötter and R. Scholz, "Digital simulation of nonlinear circuits by wave digital filter principles," in *IEEE Int. Symposium Circuits and Systems (ISCAS)*, June 1989, vol. 1, pp. 720–723.

[6] T. Felderhoff, "A new wave description for nonlinear elements," in *IEEE Int. Symposium on Circuits and Systems*, Sep. 1996, vol. 3, pp. 221–224.

[7] A. Sarti and G. De Poli, "Toward nonlinear wave digital filters," *IEEE Trans. Sig. Process.*, vol. 47, no. 6, pp. 1654–1668, June 1999.

[8] G. De Sanctis, A. Sarti, and S. Tubaro, "Automatic synthesis strategies for object-based dynamical physical models in musical acoustics," in *Proc. Int. Conf. Digital Audio Effects (DAFx-03)*, Sep. 2003, pp. 198–202.

[9] R. C. D. Paiva, S. D'Angelo, J. Pakarinen, and V. Välimäki, "Emulation of operational amplifiers and diodes in audio distortion circuits," *IEEE Trans. Circuits and Systems II: Express Briefs*, vol. 59, no. 10, pp. 688–692, Oct. 2012.

[10] M. Karjalainen and J. Pakarinen, "Wave digital simulation of a vacuum-tube amplifier," in *IEEE Int. Conf. Acoustics, Speech and Sig. Process. (ICASSP)*, 2006, pp. 153–156.

[11] S. D'Angelo, J. Pakarinen, and V. Välimäki, "New family of wave-digital triode models," *IEEE Trans. Audio, Speech, and Lang. Process.*, vol. 21, no. 2, pp. 313–321, Feb. 2013.

[12] T. Schwerdtfeger and A. Kummert, "A multidimensional approach to wave digital filters with multiple nonlinearities," in *Proc. Eur. Sig. Process. Conf. (EUSIPCO)*, Lisbon, Portugal, Sep. 2014, pp. 2405–2409.

[13] S. Petrausch and R. Rabenstein, "Wave digital filters with multiple nonlinearities," in *Proc. Eur. Sig. Proc. Conf. (EUSIPCO)*, Vienna, Austria, Sep. 2004, vol. 12.

[14] S. Bilbao, *Wave and Scattering Methods for Numerical Simulation*, J. Wiley, Ltd, New York, July 2004.

[15] J. Parker, "A simple digital model of the diode-based ring-modulator," in *Proc. Int. Conf. Digital Audio Effects (DAFx-11)*, Paris, France, Sep. 2011, vol. 14, pp. 163–166.

[16] J. J. Ebers and John L. Moll, "Large-sig. behavior of junction transistors," *Proc. of the IRE*, vol. 42, no. 12, pp. 1761–1772, Dec. 1954.